Experiments in Fluids 16, 181–186 (1994)

Experiments in Fluids

A novel flying hot-wire system

R. M. Kelso[1], T. T. Lim[2], A. E. Perry[3]

[1] CSIRO Division of Building, Construction and Engineering, P.O. Box 56, Highett, Victoria, Australia, 3190
[2] Department of Mechanical & Production Engineering, National University of Singapore, 10 Kent Ridge Crescent, Singapore 0511
[3]Department of Mechanical & Manufacturing Engineering, The University of Melbourne, Parkville, Vic., Australia, 3052.

Received: 22 June 1992 / Accepted: 21 September 1993

Abstract. A new flying hot-wire system has been developed for the measurement of highly turbulent and reversing flows. The apparatus is of rectilinear design, incorporating many features which extend its range of application beyond the range of previous designs. One of the advantages of this system is that it is mounted on a flow visualization wind tunnel which allows complementary qualitative and quantitative studies to be performed. This system has been used successfully to measure turbulent and reversing flows including the flow past a fence. Some results are presented.

List of symbols

H	height of fence
LED	light emitting diode
ST1	Schmitt trigger input signal
u, v	velocity components in the x and y directions respectively
$\langle u \rangle$, $\langle v \rangle$	phase-averaged components of u and v
x, y	orthogonal coordinate system with the x-direction aligned with the centreline along the tunnel floor and the y-component normal to the floor

1 Introduction

Accurate measurement of highly turbulent and reversed flows has historically been limited due to the inability of the measurement techniques to tolerate wide fluctuations in flow angle and, in particular, flow reversal. Techniques such as laser Doppler anemometry overcome these problems using frequency shifting techniques, but suffer from other shortcomings. Pulsed wire anemometry, although capable of measuring wide deviations in flow angle, is relatively inaccurate. Particle image velocimetry is capable of resolving reversed flows. However, the technique is not sufficiently well developed to measure turbulence quantities with accuracy. Stationary crossed wire measurements offer high accuracy in flows with low turbulence intensity, but are very limited in the range of flow angle which can be measured accurately.

Correspondence to: T. T. Lim

One way to extend the range of application of crossed wire anemometry is to move the probe at high speed against the mean flow in the wind tunnel. With a sufficiently high speed, reversed and highly turbulent flow regions will be seen by the flying probe as small perturbations, thus allowing the probe to measure with great accuracy. This has been clearly demonstrated by the whirling arm flying hot-wire of Cantwell and Coles (1983), the rectilinear designs of Watmuff, et al. (1983) (see also Perry and Watmuff (1981)) and Perry and Tan (1984) and the novel mechanism of Thompson and Whitelaw (1984). These systems allowed the turbulent wakes behind several bluff bodies to be measured accurately for the first time.

Unfortunately, the above whirling arm and rectilinear systems were limited in their range of application. For example, to conduct measurements in a strong jet in cross-flow where the jet velocity is higher than the tunnel free-stream velocity, the bias velocity of the probe needs to be many times greater than the free-stream velocity in order to limit the flow angle relative to the wires, or cone angle, to an acceptable range. In this type of flow, these systems would not allow sufficient time for the wake of the probe to leave the measurement region of the tunnel before each successive pass of the probe, thus leading to the wake contamination of the results. In fact, even in bluff body wake surveys, the choice of bias velocity involves a trade-off between the cone angle and the length of the uncontaminated measurement region. This problem was successfully avoided by Thompson and Whitelaw (1984), whose mechanism was capable of holding the probe outside the measurement region until any disturbances were convected away.

The novel flying hot-wire system described in this paper offers the convenience of a rectilinear design, which allows very large regions of the flow to be 'scanned' by the probe using a rectangular data grid, without the problem of wake contamination. Wake contamination is prevented by the introduction of a time-delay between each pass of

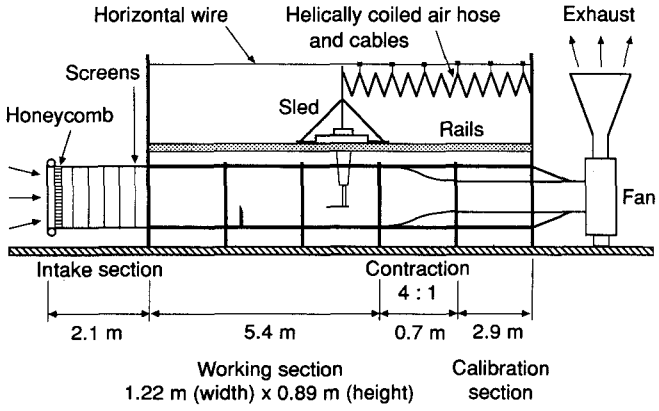

Fig. 1. Schematic diagram of the flow visualization smoke tunnel and flying hot-wire system, seen in elevation

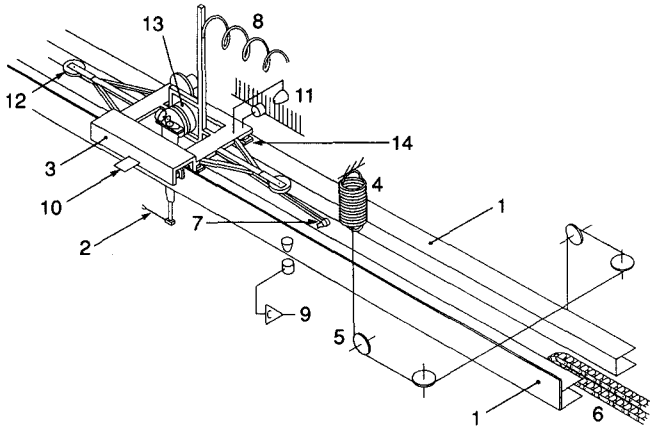

Fig. 2. Schematic layout of the new flying hot-wire system. *1* Rails, *2* Probe, *3* Sled, *4* Tension spring, *5* Pulley, *6* Slow chain, *7* Claw, *8* Air hose & cables, *9* Start-sample LED-photodetector, *10* Start-stop photodetector trigger plate, *11* Speed & position LED-photodetector, *12* Bumper pulley, *13* Cycloidal drive calibrator, *14* Air bearing pad

the probe. The time-delay is chosen to allow the probe's wake to convect from the measurement region before each pass. As a result, bias velocities far greater than the free-stream velocity can be used without wake contamination.

The new system is mounted on a flow visualization wind tunnel which allows direct comparison between qualitative and quantitative results. This apparatus also incorporates many features such as an on-board calibration system and is also capable of carrying cameras to enable flows to be observed from different frames of reference.

2 Apparatus

Figures 1 and 2 show the schematic layout of the new flying hot-wire system which is mounted on the roof of the large flow visualization wind tunnel at the University of Melbourne. The hot-wire probe is attached to a sting which is fastened to an air bearing sled sliding freely on rails above the working section. The sting passes through a slot in the roof of the tunnel which is sealed with novel plastic flaps. The sled is propelled back and forth by a spring-catapult system at the downstream end and return springs at the other end. A detailed description of this apparatus is given in Kelso, et al. (1993).

2.1 The air bearing sled

The air bearing rails consist of two horizontal rails and one vertical guide rail as shown in Fig. 2. The sled consists of a tubular steel and aluminium frame, supported at each corner by air bearing pads and guided by similar pads on either side of a vertical guide rail. The bearings are supplied with high pressure air by a long helically-coiled air hose which slides freely along a horizontal wire stretched above the tunnel. Hot-wire leads and other electrical leads are attached to this hose.

Previous rectilinear flying hot-wire designs, with the exception of the system described by Perry and Tan (1984) in which elegant but rather complex and time-consuming 'bootstrap' calibrations were performed, required the hot-wire probe to be calibrated using a separate calibration device or wind tunnel before being transferred to the sled's sting for the flying measurements. This procedure can lead to probe misalignment, hot-wire drift and even hot-wire filament breakage if extreme care is not exercised. The new sled incorporates a dynamic calibration system (see Perry (1982)), where the entire sting-traverse assembly is mounted on a mechanical shaker fitted to the sled. Using this arrangement the entire experiment, including calibrations, can be performed without handling the probe or altering its alignment. The calibrator and strut are rigidly locked during flying experiments, allowing the sting to be traversed by a stepper motor.

2.2 The propulsion mechanism

The propulsive and return spring assemblies are similar to the non-linear spring system used by Watmuff et al. (1983) except that the new system uses pulleys to confine the springs to rectilinear motion only. This results in a reduction in vibration as well as impulses and jerks on the sled. 'Bumper' pulleys are mounted on struts at both ends of the sled to engage the cables of the spring systems. These pulleys prevent the spring systems from generating any transverse thrust on the bumpers if the springs differ in stiffness.

As noted earlier, some previous flying hot-wire systems were limited in their range of application by the problem of wake contamination. One of the features of this new system is that the motion of the sled can be

controlled to prevent this occurrence when high bias velocities are used. For example, in the experiments reported in Section 5, the free-stream velocity of the wind-tunnel was typically 2 ms^{-1}, yet the bias velocity of the sled was typically 4.8 ms^{-1}. A freely reciprocating design, such as that described by Watmuff et al. (1983), would have suffered from severe wake contamination under these circumstances. The new system, however, overcomes this problem by introducing time delays in the cycle of sled motion.

The system, shown schematically in Fig. 2, is driven by a continuously moving chain drive mounted at the downstream end of the tunnel. At the end of its return stroke, the sled simultaneously contacts the return spring cable and engages the chain drive by means of a claw. The chain pulls the sled against the spring-cable system, storing strain energy, before the claw is mechanically disengaged and the sled is released. The release point is determined by the length of a steel plate, resulting in extremely repeatable release speeds. The typical release speed of the sled is 5 ms^{-1} although speeds of up to 8 ms^{-1} are possibe.

To prevent wake contamination, the chain drive speed was chosen to provide a four second time delay at the downstream end compared with a freely reciprocating sled. This delay can be increased by stopping the chain drive motor for a predetermined time using a timer connected to an external trigger. The sled was also fitted with friction brakes at the upstream end of the tunnel to reduce the return speed, typically to 3 ms^{-1}, further decreasing the possibility of wake contamination. The resulting measurement cycle takes approximately 11 seconds at a sled release speed of 5 ms^{-1}.

With this novel firing mechanism, the flying how-wire system is capable of operating at higher bias to free-stream velocity ratio than any previous rectilinear systems. Without these features the accurate measurement of the flow around a fence reported in Sect. 5 would not have been possible.

3 Hot-wire anemometry and data acquisition

3.1 Hot-wire anemometry

Unlinearized constant temperature hot-wire anemometers as described by Perry and Morrison (1971) were used throughout the experiments. Some components in the anemometers were upgraded for higher performance. The crossed wires were calibrated both statically and dynamically according to the method described in Perry (1982). This method used the on-board dynamic calibration system to oscillate the probe. To provide an adequate calibration velocity range, a 1:4 contraction followed by a high speed (0 to 14.4 ms^{-1}) calibration section were installed in the downstream part of the tunnel. Slots were incorporated into the centre of the section to allow the strut, sting and probe to pass without interference during the experiments. The slots were filled and sealed during calibrations.

Experiments such as the one described in Sect. 5 were approximately 30 hours in duration, leading to the potential for hot-wire drift. To account for this the hot-wire probe was calibrated before and after the experiments and the temperature and pressure were strictly monitored throughout. In spite of the duration, the D.C. drift in the calibrations was small, averaging 1.7%, with the worst being 3.7% of the mean velocity measured relative to the wires. As discussed by Watmuff et al. (1983), the error caused by the drift was manifested as discontinuities from level to level. To minimize this effect, the calibration constants used for each level were linearly interpolated on the basis of time.

3.2 The data acquisition system

The data are collected by a digital computer interfaced to a data acquisition unit which is controlled by three LED-photodetector pairs through the Schmitt trigger inputs, as outlined by Watmuff et al. (1983). Samples are taken at predetermined spatial intervals along the length of the working section. The 'start' and 'stop' photodetectors are fixed to the tunnel at each end of the working section. They are triggered by a metal plate fixed to the sled. The third photodetector is used to monitor the position of the hot-wires along the tunnel. Attached to the sled, it rides past a fixed grating to produce one Schmitt trigger (STI) pulse per millimetre of travel. These pulses are used by the computer to register the position of each sample of data. This allows measurements to be taken at 1 mm intervals if required. The frequency of the ST1 pulses give the speed of the sled in $mm\,s^{-1}$.

Most of the software used in this work is based on the software described by Watmuff et al. (1983), but modified to account for some difference between the data acquisition systems and sampling rates. The data presented in this paper were acquired by a Digital PDP 11/10 computer, although the system has since been interfaced with an IBM compatible personal computer.

The phase sampling and sorting were controlled by a 'phase pulse' which was obtained from a mechanical forcing mechanism. The operation of the entire flying hot-wire system, including the phase sampling system, was tested using the barber's pole method of Perry and Steiner (1987).

4 Application to a flow behind a fence

The new flying hot-wire system was used to conduct time-averaged and phase-averaged velocity and global turbulence measurements behind a fence. Some of the phase-averaged results are presented here.

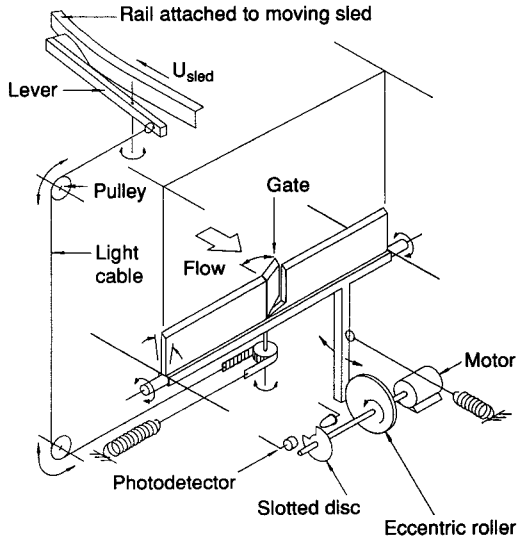

Fig. 3. Schematic diagram of the gate opener and the fence shaker

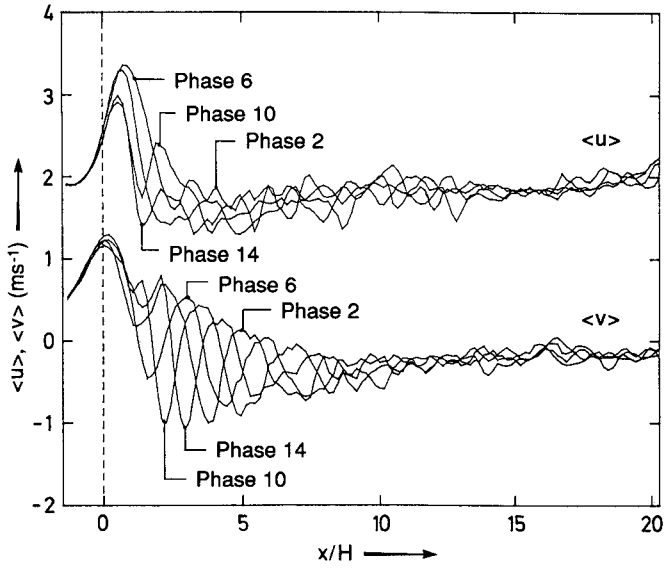

Fig. 4. Phase-averaged velocity signatures obtained during the forced fence experiments. Phases 2, 6, 10 and 14 are shown

The experimental set-up consisted of a nominally two-dimensional fence, 190 mm (H) high, mounted spanwise across the floor of the working section of the wind-tunnel. Phase-averaged velocity measurements were made on the vertical centreline plane at a horizontal grid spacing of 32 mm (115 or 130 stations depending on height) and a vertical grid spacing of 22 mm (20 levels). The data were collected over 400 passes of the sled at each level and sorted into 16 equal phase intervals. This resulted in an average of 25 samples per phase per sampling station. The Reynolds number was approximately 26,000 based on the fence height and the free-stream velocity of 2.05 ms^{-1}. The bias velocity of the sled was approximately 4.8 ms^{-1}. The upstream boundary layer was perturbed to give a turbulent profile of 65 mm thickness.

To improve the periodicity of the shear layer roll-up for the purposes of phase-averaging, the fence was hinged about its junction with the floor and shaken by an eccentric roller as shown in Fig. 3. A 'phase pulse', which was used to detect the phase of the forcing input, was generated by a photodetector which was triggered by a slotted disc mounted on the same shaft as the roller. The amplitude and frequency of forcing were controlled by adjusting the eccentricity of the roller and varying the speed of the shaker respectively. A forcing frequency of 3.2 Hz was chosen to match the vortex passage frequency over the central region of the unforced separation bubble. The choice of the amplitude of the forcing (1.7°) was based on both flow visualization studies and stationary hot-wire measurements.

In order to measure the separation region close to the rear surface of the fence, a gate was incorporated in the fence to allow the probe to pass through at high speed without damage, as shown in Fig. 3. Arrangements were made to ensure the gate and the fence were properly sealed. When the probe was sampling above the fence, the gate opener was disconnected and data were sampled upstream of the fence.

4.1 Results

All the data presented in this paper were multi-point smoothed according to the methods described in Watmuff et al. (1983).

Figures 4 shows the phase-averaged u- and v-velocity signatures along level 14 of the measurement grid. The position of the fence is marked by a dashed vertical line. Only phases 2, 6, 10 and 14 are shown, and the data were 3-point smoothed. In the near field between the fence and the reattachment point ($x/H = 8.4$) there is strong coherence in the velocity signatures, particularly in the v-component. The amplitude of the waveforms decays very rapidly near reattachment whereupon the waveforms become subject to considerable phase jitter and noise. It is believed that this effect is largely due to the increasing jitter of the forced shear layer brought about by vortex interactions such as pairing. Note also that the u-signatures have a smaller amplitude since the measurements were taken near the middle of the shear layer.

Figure 5 shows the velocity vector field and streamline pattern for one phase as seen by an observer moving with the convection velocity of the second eddy, which is approximately 1.65 ms^{-1}. The velocity data were five-point smoothed along the rows and columns. This pattern represents an phase-averaged picture of the flow at one stage of the forcing cycle. Superimposed on the vector field is the integrated streamline pattern which was computed by

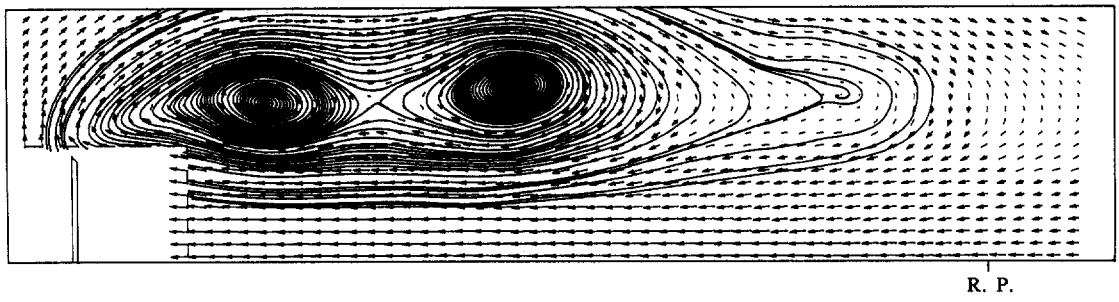

Fig. 5. Velocity field and integrated streamline pattern for one phase as seen by an observer moving at the convection velocity of the second eddy. R. P. refers to the mean reattachment position

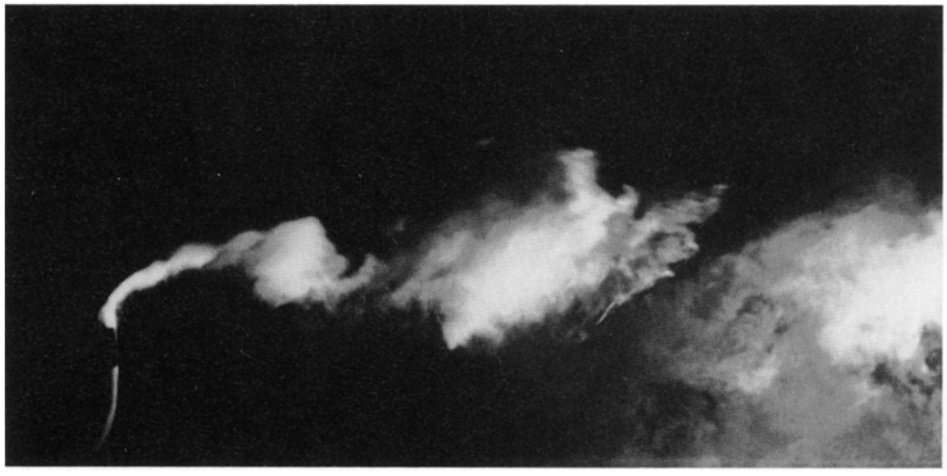

Fig. 6. Laser cross-section of the forced flow downstream of the fence. Smoke was introduced immediately behind the separation point

integrating piecewise-cubic B-spline interpolations of the velocity field. Since no velocity measurements were taken close to the fence, dummy data were extrapolated into this region to allow the cubic spline software to operate correctly. The convection velocity was calculated using a method based on the vortex celerity method of Cantwell and Coles (1983). In this figure, all three eddies appear as stable foci in the large. This flow pattern is interesting in that the first and second eddies exhibit very slow rates of spiralling in, which indicates that the flow is very close to two-dimensional. The third eddy, which was washed-out by the effects of jitter, appears to be stable focus with a large radial velocity.

4.2 Cone angles

The most significant advantage of flying hot-wires over stationary hot-wires is the reduction in the cone angle of the flow relative to the probe. Studies by the present authors (not included here) show that the 90° cross-wires used in these experiments will deliver accurate measurements up to an angle of $\pm 20°$ to the axis of the probe in the plane of the wires. This has also been shown by Perry et al. (1983).

The phase-averaged results show that the largest cone angles were encountered by the flying probe near the tip of the fence and they varied between 15.5° and 18.4° over the forcing cycle. Amplitude jitter will lead to excursions beyond this range but these excursions are likely to be small, given the periodic nature of the flow in this region. If the same crossed wire probe were stationary at the same location, it would encounter cone angles varying between 48° and 54°, neglecting the effects of jitter.

Phase-averaged cone angles encountered in the shear layer were typically within $\pm 8°$ for the flying probe, compared to $\pm 26°$ for a stationary probe. In the reversed flow region beneath the shear layer (i.e. a cone angle of 180° relative to a stationary probe), the phase-averaged cone angles encountered by the flying probe were within $\pm 5°$.

The above results are significant since they illustrate the power of the flying hot-wire method to obtain accurate velocity and turbulence measurements in regions of large angular deviation, high turbulence intensity and reversed flow. With a flying hot-wire there is no necessity for probe alignment with the local mean flow direction and the problems of high turbulence intensity can be eliminated, provided the bias velocity of the probe is high enough.

4.3 Flow visualization studies

A further advantage of this facility is that it is mounted on a flow visualization tunnel allowing both qualitative and quantitative studies to be performed. To complement the hot-wire measurements presented above, flow visualization studies were carried out using the laser cross-sectioning technique utilizing a 5 Watt Argon-Ion laser with a glass rod as a beam spreader. Smoke was injected into the separating shear layer from the downstream side of the fence. The operating conditions were the same as in the quantitative study. Figure 6 shows a typical laser section photograph of the flow behind the fence which corresponds reasonably well to the instantaneous streamline pattern of Fig. 5.

5 Discussion and conclusions

The novel flying hot-wire system described here represents a major advance in versatility and accuracy over previous rectilinear systems due to both the on-board calibration system and the avoidance of wake contamination. It has already proven to be a powerful tool for the measurement of turbulent shear flows and, in particular, reversing and highly three-dimensional flows. The fact that this facility is mounted on a flow visualization tunnel makes it ideal for the study of flow topology. This system has enabled the unsteady flow behind a fence to be accurately and comprehensively studied. The system has also been used successfully to measure a strong jet in cross-flow. These results will be reported elsewhere.

Acknowledgements

The authors wish to acknowledge the financial assistance of the Australian Research Council. The first author acknowledges the support of the CSIRO.

References

Cantwell, B.; Coles, D. 1983: An experimental study of entrainment and transport in the turbulent near wake of a circular cylinder. J. Fluid Mech. 136, 321–374

Kelso, R. M.; Lim, T. T.; Perry, A. E. 1993: A novel flying hot-wire system. Report No. FM-21, University of Melbourne

Perry, A. E. 1982: Hot-wire anemometry, Clarendon Press, Oxford

Perry, A. E.; Lim, K. L.; Henbest, S. M.; Chong, M. S. 1983: Rough- and smooth-walled shear flows. Proc 5th International Symposium on Turbulent Shear Flow, Cornell U.S.A.

Perry, A. E.; Morrison, G. L. 1971: Static and dynamic calibration of constant-temperature hot-wire systems. J. Fluid Mech. 47, 765–777

Perry, A. E.; Steiner, T. R. 1987: Large-scale vortex structures in turbulent wakes behind bluff bodies. Part 1. Vortex formation processes. J. Fluid Mech. 174, 233–270

Perry, A. E.; Tan, D. K. 1984: Simple three-dimensional vortex motions in coflowing jets and wakes. J. Fluid Mech. 141, 197–231

Perry, A. E.; Watmuff J. H. 1981: The phase-averaged large-scale structures in three-dimensional turbulent wakes. J. Fluid Mech. 103, 33–51

Thompson B. E.; Whitelaw, J. H. 1984: Flying hot-wire anemometry. Exp. Fluids 2, 47–55

Watmuff, J. H. 1979: Phase-averaged large-scale structures in three-dimensional turbulent wakes. Ph.D. Thesis, University of Melbourne

Watmuff, J. H.; Perry, A. E.; Chong, M. S. 1983: A flying hot-wire system. Exp. Fluids 1, 63–71